Boron isotope analysis of silicate glass with very-low boron concentrations by secondary-ion mass spectrometry

Horst R. Marschall[1]*, Brian D. Monteleone[1]

[1] Department of Geology and Geophysics, Woods Hole Oceanographic Institute, Woods Hole, MA 02543, USA

*Corresponding author. Tel: +1-508-289-2776. Fax: +1-457-2183. E-mail: hmarschall@whoi.edu

Short title: MORB δ^{11}B by SIMS

Submitted to **Geostandards and Geoanalytical Research** on 14. Nov. 2013
Revised version submitted on 14. Feb. 2014
Accepted for publication on 02. March 2014

This version is from 14. Feb. 2014

Abstract

Here we present an improved method for the determination of the boron isotopic composition of volcanic glasses with boron concentrations of as low as $0.4-2.5\,\mu g/g$, as is typical for mid-ocean ridge basalt glasses. The analyses are completed by secondary-ion mass spectrometry using a Cameca 1280 large-radius ion microprobe. Transmission and stability of the instrument and analytical protocol were optimised, which led to an improvement of precision and reduction of surface contamination and analysis time compared to earlier studies. Accuracy, reproducibility ($0.4-2.3\,‰$, 2RSD), internal precision ($2RSE = 2.5-4.0\,‰$ for a single spot with $[B] = 1\,\mu g/g$), matrix effects ($\ll 0.5\,‰$ among komatiitic, dacitic and rhyolitic glass), machine drift (no internal drift; long-term drift: $\sim 0.1\,‰/h$), contamination ($\sim 3-8\,ng/g$) and machine background ($0.093\,s^{-1}$) were quantified and their influence on samples with low B concentrations was determined.

The newly developed setup is capable of determining the B isotopic composition of basaltic glass with $1\,\mu g/g$ B with a precision and accuracy of $\pm 1.5\,‰$ (2RSE) by completing $4-5$ consecutive spot analyses with a spatial resolution of $30\times 30\,\mu m^2$. Samples with slightly higher concentrations ($\geq 2.5\,\mu g/g$) can be analysed with a precision of better than $\pm 2\,‰$ (internal 2RSE) with a single spot analysis, which takes 32 min.

Keywords: boron isotopes; MORB; low concentration; SIMS; ionprobe

Introduction

Boron is a moderately volatile, lithophile non-metal with a low atomic mass and two stable isotopes and a $^{11}B/^{10}B$ variation of several tens of per mil in Earth's surface environments (Palmer & Swihart, 1996). The strong enrichment of B in the crust and the significant difference in B isotopic compositions between continental crust, modern seawater and the depleted mantle make B a potentially powerful geochemical tracer for the secular evolution of the ocean-crust-mantle system (e.g., Spivack & Edmond, 1987; Chaussidon &

Marty, 1995; Turner *et al.*, 2007). However, the very low abundance of B in mantle rocks and primitive volcanic rocks confronts us with a major analytical hurdle. Boron isotope analyses of silicate materials at the trace abundance level are highly challenging. The B isotopic compositions of the Earth's major reservoirs (i.e., continental crust, primitive and depleted mantle) are still poorly constrained, despite a several decades-long history of research into B isotope geochemistry.

The pioneering work by Chaussidon and co-workers (Chaussidon & Jambon, 1994; Chaussidon & Marty, 1995; Chaussidon *et al.*, 1997) has demonstrated the capability of secondary-ion mass spectrometry (SIMS) to determine the B isotopic composition of mantle-derived lavas, and exemplified the use of B isotopes as a geochemical tool in these rocks. However, the small-radius mass spectrometers available in the 1980s and '90s have been surpassed in terms of transmission and stability by the large-radius ion microprobes available today, which provide a 3 to 5 times higher sensitivity for B isotope measurements in low-B samples (e.g., Chaussidon *et al.*, 2006; Gurenko & Kamenetsky, 2011; Shaw *et al.*, 2012, this study). Improvements have also been made in controlling and quantifying surface contamination (Marschall & Ludwig, 2004). Furthermore, the availability of new international reference materials (Gonfiantini *et al.*, 2003; Jochum *et al.*, 2006) enables a fresh assessment of the capabilities and limits of in-situ B isotope analysis by SIMS. The method presented in this paper provides the means for routine analysis of B isotope ratios in natural volcanic glasses at concentration levels from depleted MORB to highly enriched rhyolites.

Analytical setup

Boron isotope ratios were determined by SIMS using a Cameca ims1280 ion microprobe at the North-Eastern National Ionmicroprobe Facility (NENIMF) at the Woods Hole Oceanographic Institution between October 2012 and September 2013. The parameters for B isotope analyses were: $25-40\,\mathrm{nA}$, $22\,\mathrm{keV}$ $^{16}O^-$ primary ion beam; $10\,\mathrm{kV}$ secondary acceleration voltage; $\pm 40\,\mathrm{eV}$ energy window without offset; secondary ion detection by a single electron multiplier (ETP, SGE Analytical Science) in counting mode (electronically set deadtime $\tau = 28\,\mathrm{ns}$). The primary beam was tuned on an Al metal grid using a $200 \times 200\,\mu\mathrm{m}^2$ raster. The

energy distribution of the secondary beam was scanned periodically on each sample mount using the $^{28}Si^{2+}$ signal, and the energy window was centered on the maximum energy. On high-B samples (e.g., reference glass B6; see below) the energy window was centered using the $^{11}B^{+}$ signal.

A $70 \times 50\,\mu m$ raster was applied during presputtering to remove the gold layer and reduce surface contamination. Presputtering lasted for $200 - 300\,s$. Prior to each measurement, mass calibration of $^{10}B^{+}$ and $^{11}B^{+}$ was performed, and fine tuning of the secondary column deflectors, stigmators, and lenses was done manually in order to maximize the signal of $^{28}Si^{2+}$ on the electron multiplier, thereby maintaining maximum transmission throughout the session. Automatic beam centering using the $^{11}B^{+}$ signal was found to be unreliable for samples with very low B concentrations. Gaussian illumination was used, which gave high transmission of the rectangular rastered area through the square-shaped field aperture. A $4000 \times 4000\,\mu m^2$ field aperture was used to exclude the edge of the secondary beam, again reducing the influence of surface contamination (Marschall & Ludwig, 2004). The field of view of the sample through this aperture is $30 \times 30\,\mu m^2$, which defines the spatial resolution of the analysis and the ion-optical magnification ($130\times$). The largest contrast aperture ($400\,\mu m$) was used to maximise transmission. We did not systematically test other combinations of setups. No evidence for charging was found. Surface contamination is discussed below in more detail. The instrument was operated in the X-Y mode, which produced a more ideal peak shape and high transmission. No strong increase in transmission was observed when switching to circular mode. However, this could be explored more rigorously in future to possibly further increase transmission.

The analyses were performed using a rastered area of $30 \times 30\,\mu m^2$ in the centre of a larger pre-sputtered area ($70 \times 50\,\mu m^2$). It was found that performing the analyses in raster mode produces ablation pits with a flatter bottom and less depth progression compared to spot analyses, as well as more constant secondary ion signals over the duration of an analysis. The sputter rate on the basaltic glasses is $1.6 \pm 0.5\,nm/s$. Dimensions of the sputtered areas were determined using an automatic-focus Zeiss AxioImager reflected light microscope with the AxioVision imaging software including the topography package. Sputter pits created by a regular 40-cycle analysis recommended for routine work are $\sim 3.1\,\mu m$ deep, resulting in an

aspect ratio of the sputtered pits of ~ 0.1. The amount of total sputtered material during an analysis is $\sim 5.1 \times 10^3\,\mu m^3$.

No dynamic transfer setting was used in order to avoid the inclusion of the contamination-afflicted edge of the beam in the analyses. Forty cycles were measured per analysis, switching between masses $^{10}B^+$ and $^{11}B^+$. The integration times per cycle were 20 s for ^{10}B and 10 s for ^{11}B. The mass resolution $m/\Delta m$ was set to ~ 1250 at 10 % intensity ratio, which is sufficient to remove possible molecular interferences (e.g., Ludwig *et al.*, 2011). The total time required for one analysis is 32 min. This analysis time could be reduced to 22 min per spot, if a multi-collection system was used, as that would remove the settling time (a total of 5 s per cycle) and the integration time for the more abundant isotope (10 s per cycle).

The raw count rates were corrected for both the multiplier deadtime and for the slow changes in secondary ion intensity over the course of a single measurement (i.e., time interpolation). The latter was done by averaging counts of ^{10}B from two subsequent cycles and calculate the $^{11}B/^{10}B$ ratio by dividing the count rate of the intermediate ^{11}B measurement by that average. The extent of this intensity correction is typically $0.1 - 1.0$ ‰. Each analysis consisting of 40 analytical cycles, therefore, produced 39 isotope ratios. The count rates were also corrected for the machine background of $0.093\,s^{-1}$, which was determined by analysing mass 9.7 on different glass samples over the course of one week for a total integration time of 127 min. This correction is very small for natural volcanic glass, i.e. < 0.25 ‰ for MORB glasses with $[B] = 0.4\,\mu g/g$ and < 0.10 ‰ for MORB glasses with $[B] = 2.5\,\mu g/g$. Finally, the 39 isotope ratios of each analysis were filtered for statistical outliers $> 3\sigma$. These outliers are rare and are typically related to intensity jumps in the primary beam, and any such cycles were rejected. On average, one in four analysis has one cycle that is rejected. Isotope ratios calculated from averaging a number of ratios collected over the course of a single analyses are positively biased, but this bias decreases with increasing counts N of the minor isotope per measurement cycle, bias $= 1/N + 2/N^2$ (Ogliore *et al.*, 2011). The largest bias expected for the MORB glasses with the lowest B concentration ($[B] = 0.4\,\mu g/g$; ^{10}B: $N = 6500$ counts per cycle) is $+0.15$ ‰. Results were not corrected for this bias.

Boron isotopes are reported in the delta notation relative to SRM 951 (U.S. National Institute of Standards and Technology, NIST; Catanzaro *et al.*, 1970): $\delta^{11}\mathrm{B} = [(^{11}\mathrm{B}/^{10}\mathrm{B}_{\mathrm{sample}})/(^{11}\mathrm{B}/^{10}\mathrm{B}_{\mathrm{SRM\,951}}) - 1] \cdot 1000$ ($^{11}\mathrm{B}/^{10}\mathrm{B}_{\mathrm{SRM\,951}} = 4.04362$). Analytical uncertainties are discussed below.

Boron concentrations were determined using the Cameca ims1280 with the same setup for raster sizes and aperture, mass resolution, 40 nA $^{16}\mathrm{O}^-$ primary beam, and size of energy window with zero offset. Pre-sputtering lasted for 2 min. Ten analytical cycles were analysed including masses $^{11}\mathrm{B}^+$ and $^{28}\mathrm{Si}^{2+}$. Reference glass GOR132-G (Table 1; Jochum *et al.*, 2000) was used to determine $^{11}\mathrm{B}^+/^{28}\mathrm{Si}^{2+}$ relative ion yields[1], which were 490 ± 6 (2SD; n = 4) and 454 ± 20 (2SD; n = 6) for two different sessions. Reference glass B6 (Gonfiantini *et al.*, 2003; Tonarini *et al.*, 2003) was also analysed in the latter session and resulted in a relative ion yield of 435 ± 1 (2SD; n = 2), which is indistinguishable from the result on GOR132-G in that session.

Reference materials and samples

Four different reference materials were used in this study, as given in Table 1. This includes natural glass and glasses prepared from natural volcanic rocks. Glass compositions range from komatiitic to rhyolitic, with boron concentrations of approximately $12 - 200\,\mu\mathrm{g/g}$ (Table 1). GOR128-G and GOR132-G belong to the set of MPI-DING glasses and were prepared from Gorgona (Columbia) komatiite samples GOR128 and GOR132, respectively (Jochum *et al.*, 2000). Boron concentrations and $^{11}\mathrm{B}/^{10}\mathrm{B}$ ratios in these glasses are much higher than expected for mafic or ultramafic volcanic rocks and point to assimilation of seawater-altered materials into the Gorgona magmas (Jochum *et al.*, 2006). The high abundance of B ($\sim 20\,\mu\mathrm{g/g}$; Table 1) makes these glasses well suite as SIMS reference materials.

Reference material StHs6/80-G is another MPI-DING glass that was prepared by melting and quenching a sample of dacitic ash from Mount St Helens (Washington, USA). It has a moderately high abundance of B and a B isotopic composition that is similar to that of mid-ocean ridge basalts (Jochum *et al.*, 2000, 2006).

[1] $\mathrm{RIY} = {}^{11}\mathrm{B}^+/{}^{28}\mathrm{Si}^{2+} \cdot [\mathrm{Si}]/[\mathrm{B}] \cdot (\bar{\mathrm{M}}_{\mathrm{B}}/\mathrm{I}_{11_{\mathrm{B}}})/(\bar{\mathrm{M}}_{\mathrm{Si}}/\mathrm{I}_{28_{\mathrm{Si}}})$; $\bar{\mathrm{M}}$ = mean atomic mass, I = isotopic abundance.

Reference material B6 is a natural obsidian glass from Lipari island (Aeolian archipelago, Italy) that was characterised in a B isotope interlaboratory comparison study (Gonfiantini *et al.*, 2003; Tonarini *et al.*, 2003). The material is distributed by the International Atomic Energy Agency (IAEA). Its boron abundance is the highest of all materials investigated here ($\sim 200\,\mu g/g$; Table 1), which allows low-uncertainty SIMS analysis of this reference material. The interlaboratory study resulted in δ^{11}B values determined by P-TIMS of -3.35 ± 0.24‰, -1.56 ± 0.60‰, and -0.45 ± 0.60‰ (mean $\delta^{11}\mathrm{B} = -1.79 \pm 2.93$‰).

NIST glasses SRM 610 or SRM 612 were not used to determine the instrumental mass fractionation (IMF), as they have been demonstrated to produce IMF values that are different from all silicate glasses with natural compositions, and that that difference depends on machine type and setup (Rosner *et al.*, 2008; Gurenko & Kamenetsky, 2011).

All glass samples analysed in this study were large fragments ($0.5 - 2$ mm diameter) that were mounted in epoxy (Buehler Epothin) or pressed into indium mounts within 7 mm radius of the centre of the 12.7 mm radius sample holder. Indium mounts generally produce a lower background during SIMS volatile analyses, whereas it may be easier to produce a sample surface that is flat across the entire mount if the samples are embedded in epoxy. It is neither expected nor observed that the epoxy should influence the machine background for boron; however, the mounting materials were not systematically evaluated against each other in the course of this study. The epoxy was annealed in a pressure chamber at 400 kPa to suppress the formation of bubbles that would potentially disturb the surface and the stability of the vacuum. Polishing was completed using a Buehler MiniMet 1000 polishing machine (1 µm diamond paste), which was set to produce a flat and even surface throughout the epoxy and glass samples. Alumina polish (0.3 µm) was used for the final polish. It was found that polishing new epoxy mounts within the first few weeks leads to a relatively strong relief around the edges of the samples, while waiting several months before the final stage of polishing leads to further hardening of the epoxy, and a very flat surface can be produced. Flat surfaces without relief, pits or cracks are essential for accurate isotope measurements by SIMS (see discussion in Kita *et al.*, 2009, for O isotopes).

No systematic investigation of surface flatness on the measured B isotope ratio was conducted here. However, we analysed one glass sample that was in contact with two large exposed epoxy gas bubbles (~ 0.5 mm diameter; see supplementary figure) at various distances to the gas bubbles to investigate the possible influence of surface discontinuity. No systematic difference was found between analyses close to a gas bubble ($< 200\,\mu$m) compared to analyses at large distances from any gas bubble ($\sim 600 - 1000\,\mu$m; supplementary figure). This demonstrates that the B isotope measurements in our analytical setup are more robust against surface discontinuities than O isotope analyses.

All analysis were completed at a distance of at least 100 µm from the edge of the samples. This includes the reference materials and MORB glasses. Prior to gold coating, the grain mounts were cleaned using 96 % ethanol followed by an ultrasound bath using distilled water from a Millipore ultrapure water system (18 MΩ). The Millipore system typically reduces the B concentration in the water to $< 0.5\,\mu$g/L (from $\sim 40\,\mu$g/L in tap water; Darbouret & Kano, 2000). Samples were always cleaned and coated immediately before introducing them into the airlock of the mass spectrometer to reduce the possible deposition of contamination on the sample surfaces.

Contamination

In general, thin sections and polished grain mounts are used for the analysis of B concentrations and B isotopic compositions by SIMS. The surfaces of these samples are prone to the collection of contamination with boron-bearing and other volatile or water-soluble compounds during sample preparation and during storage (Shaw *et al.*, 1988; Chaussidon *et al.*, 1997; Hervig, 2002; Marschall & Ludwig, 2004). Surface contamination has also been demonstrated to exist for Li, Na, K and Fe (Müller *et al.*, 2003; Marschall & Ludwig, 2004), but is particularly recognised as a significant obstacle in the determination of accurate B abundance and B isotope data in low-B concentration samples (Shaw *et al.*, 1988; Chaussidon *et al.*, 1997; Marschall & Ludwig, 2004). Levels of contamination may depend on the techniques of sample preparation and cleaning procedures used, as well as analytical procedures during SIMS analysis. Additional

contamination may be produced during analysis by implantation of boron through the primary beam from low-purity materials in the duoplasmatron (Chaussidon *et al.*, 1997). However, this is avoided by primary beam mass filtering in modern SIMS instruments. Significant memory effects, as is potentially the case with laser-ablation-ICP-MS (see discussion in le Roux *et al.*, 2004), have not been observed in SIMS, except after sputtering boron-rich salts (Chaussidon *et al.*, 1997). Estimates for the equivalency of surface contamination plus instrumental background contamination range from $< 10\,\mathrm{ng/g}$ (Kent & Rossman, 2002; Marschall & Ludwig, 2004) to $10-50\,\mathrm{ng/g}$ (Chaussidon *et al.*, 1997) to $\geq 2\,\mu\mathrm{g/g}$ (Domanik *et al.*, 1993; Marschall & Ludwig, 2004).

A large range of minerals and glasses that are of geological interest show B abundances below $10\,\mu\mathrm{g/g}$, and many show abundances of approximately $1\,\mu\mathrm{g/g}$ (e.g., Ottolini *et al.*, 2004; Marschall *et al.*, 2006*a*). For example, mid-ocean ridge basalt (MORB) glasses commonly contain $0.4-2.5\,\mu\mathrm{g/g}$ (Spivack & Edmond, 1987; Ryan & Langmuir, 1993; Chaussidon & Jambon, 1994; Leeman & Sisson, 2002; le Roux *et al.*, 2004). Boron surface contamination is, therefore, potentially significant for these type of samples, and its suppression is imperative in order to reduce bias in B abundance and isotope measurements. Moreover, it is critical to quantify the amount and B isotopic composition of the remaining surface contamination, so that an estimate can be made of the bias introduced by the remaining contamination.

Here, we use the silica glass Herasil-102 (Heraeus Quarzglas GmbH, Germany) to characterise B surface contamination. Herasil-102 was recommended as an appropriate material to quantify B surface contamination, as it is an ultrapure, homogeneous material that is available in large quantities, and its B concentration is $\leq 1.1\,\mathrm{ng/g}$ (Marschall & Ludwig, 2004). Any ion signals of $^{10}B^{+}$ and $^{11}B^{+}$ detected by the multiplier during a regular measurement on Herasil-102 can be attributed to the combined contributions of surface contamination, machine background, memory effects and B from the glass itself. Importantly, the abundance of B in Herasil-102 is very low, so that the contributions from the other sources become dominant and can be evaluated. A fragment of Herasil-102 was mounted in epoxy and polished together with the B isotope reference materials and a number of MORB glasses and analysed for apparent B concentration and

B isotopic composition along with these samples using the same analytical setups.

Boron isotope measurements on Herasil-102 resulted in ion yields of $\sim 25\,s^{-1}$ for ^{11}B. In MORB glasses with B concentrations of $0.4-2.5\,\mu g/g$, the same count rate amounts to a contamination contribution of $8\,ng/g$ or $0.3-2.0\,\%$ to the total counted signal. The B isotopic composition of the surface contamination using Herasil-102 can only be determined with large uncertainty, due to the very low count rates. Four analyses were completed and resulted in $\delta^{11}B$ values ranging from $-58\pm71\,‰$ to $+2\pm45\,‰$, with a mean of $-36\pm27\,‰$ (2SE). These values are used to estimate the systematic error of B surface contamination on the B isotope analyses of the samples using a simple mass balance approach:

$$\delta^{11}B_d = X_s \cdot \delta^{11}B_s + X_c \cdot \delta^{11}B_c \quad (1)$$

where $\delta^{11}B_d$ is the determined B isotope value (measured value corrected for intensity and instrumental mass fractionation), $\delta^{11}B_s$ is the the true value of the sample, and $\delta^{11}B_c$ is the B isotope value of the contamination. X_s and X_c are the proportions of B from the sample and the contamination that contribute to the signal ($X_s + X_c = 1$).

The bias for the determined B isotope value introduced from contamination, i.e. the difference between $\delta^{11}B_d$ and $\delta^{11}B_s$ is displayed in Fig. 1a, assuming $\delta^{11}B_s = -7\,‰$ for the sample and a contamination $\delta^{11}B_c = -36\,‰$ as discussed above. Note that the absolute values plotted in Fig. 1 depend on the difference between $\delta^{11}B_s$ and $\delta^{11}B_c$.

MORB glass samples measurements with a $0.3-2.1\,\%$ signal contribution from contamination would have to be corrected by $+0.09$ to $+0.23\,‰$ to retrieve the uncontaminated isotopic composition of the sample (Fig. 1). However, this systematic error has a large uncertainty, due to the large uncertainty of the isotopic composition of the contamination component (Fig. 1) and, thus, no contamination correction of the $\delta^{11}B$ values was done during this study.

Furthermore, the systematic error introduced by contamination can be estimated as a function of B con-

centration of the analysed sample for the specific setup used in this study using Equation 1. In this case, X_c is derived from the apparent B concentration of the contamination $[B]_c = 8\,ng/g$ and $[B]_s$, the true B concentration of the sample: $X_c = [B]_c/([B]_s + [B]_c)$. The model demonstrates that for our analytical setup the potential systematic error introduced by contamination is only $0.23\,‰$ for a sample with a B concentration of $1\,\mu g/g$, or $0.58\,‰$ ($\pm 2SE = 0.04 - 1.11\,‰$) for $0.4\,\mu g/g$ samples (Table 2; Fig. 1b). Larger biases would be expected for samples with much lower B contents or with exotic B isotopic compositions that diverge more from that estimated for the contamination.

Precision

The internal precision of a single spot analysis is defined here as the standard error of the mean ($SE = SD/\sqrt{n}$) of the $n = 39$ intensity-corrected $^{11}B/^{10}B$ ratios and are given here as two times the relative standard error[2]. In practice, the precision will depend on counting statistics, on the homogeneity of the analysed material on the scale of the measurement (micrometres in the case of SIMS), on surface contamination, on the stability of the mass spectrometer and the detector system, and, especially in case of a single-collector measurement, on the stability of the primary beam. At low concentrations, the standard error is dominated by counting statistics and can be predicted from Poisson statistics in a contamination-free measurement (e.g., Fitzsimons *et al.*, 2000):

$$RSE(‰) = 1000 \cdot \sqrt{\frac{1}{\sum N_{10}} + \frac{1}{\sum N_{11}}}, \tag{2}$$

where $\sum N_{10}$ and $\sum N_{11}$ are the total counts of ^{10}B and ^{11}B, respectively, over the course of the analysis. For example, in a sample containing $1\,\mu g/g$ B, the count rates of ^{10}B and ^{11}B may be $3200\,s^{-1}$ and $800\,s^{-1}$, respectively, translating to 6.4×10^5 and 1.28×10^6 counts, respectively, for this analysis. The predicted precision is $2RSE = 3.06\,‰$. Measurements that are significantly afflicted with surface contamination show

[2]Note that all errors and uncertainties discussed in this paper are 2 standard deviations or 2 standard errors, while previous publications in many cases report 1 RSD and 1 RSE uncertainties.

decreasing count rates over the course of the analysis and have a precision that is many times worse than statistically predicted (Marschall & Ludwig, 2004).

The sensitivity of the instrument, i.e., the number of counts per second registered during an analysis of a sample with a given concentration, depends on the setup of the instrument (mass resolution, energy filtering, etc.), on the primary beam current (or more specifically on the product of beam density and analysed area) and on the ion yield. The last is relatively constant among basaltic glasses, but may vary significantly (i.e., a factor of 2) between basaltic and rhyolitic glasses. In our study, the sensitivity varied between approximately 50 and 80 counts/s/nA/(μg/g) for ^{11}B on the GOR glasses. The resulting predicted precisions for primary beam currents of 25 and 40 nA are displayed in Fig. 2. This figure also shows the precision of analyses of the reference materials and a range of MORB glasses. Observed and predicted precisions agree well at low concentrations, while counting statistics is not the limiting factor at concentrations $> 20\,\mu g/g$ where the internal precision reaches a practical lower limit of $\sim 0.5\,‰$ (2RSE). This practical limit is likely set by the stability of the primary beam and of the ablation and ionisation conditions. These factors are much less effective when both ions are counted simultaneously. The practical limit of precision may therefore be lower on a multi-collector instrument. The majority of MORB glasses ($[B] = 0.4 - 1.2\,\mu g/g$) were analysed with a precision of between 2.5 and 4 ‰ (2RSE; Fig. 2).

The sensitivity of the instrument may also be expressed in terms of the useful ion yield (Hervig *et al.*, 2006), which depicts the number of counted ions of a particular isotope relative to the number of sputtered atoms of that isotope. For example, basaltic glass (assumed density = 2700 kg/m^3) with $[B] = 1\,\mu g/g$ ($^{11}B/^{10}B = 4$) contains 1.2×10^5 atoms/μm^3 of ^{11}B. Our analytical setup (sputter rate 1.65 nm/s; sputtered area $30 \times 30\,\mu m^2$) consumes $1.48\,\mu m^3/s$ ($= 4$ pg/s) of basalt glass. The amount of sputtered ^{11}B is, therefore, 1.78×10^5 atoms/s. The count rate on such a sample is typically $3200\,s^{-1}$. Hence, our useful ion yield is 1.8 %. This is approximately one order of magnitude higher than the useful ion yields reported for boron for small-radius ion microprobes (Cameca 3f and 6f), which range from 0.14 to 0.31 % (Hervig *et al.*, 2006). The total amount of boron consumed during a 32 min analysis of a $[B] = 1\,\mu g/g$ glass including the

larger-area pre-sputtering is 14 fg from 14 ng of glass.

The precision of the measurement improves with the amount of boron consumed, which increases with integration time and the number of analytical cycles for a given sample (Fig. 3). The analytical setup used in this study permits MORB glasses with B concentrations of $1\,\mu g/g$ to be analysed with an observed precision of $\sim 2.5-4.0\,‰$ (2RSE), which agrees with the Poisson statistical prediction of $3.1\,‰$. This internal precision compares very favourably with previous studies using various SIMS and laser-ablation inductively-coupled-plasma (LA-ICP-MS) instruments (Table 2).

Analysis of homogenous basaltic glass with $1\,\mu g/g$ B require ~ 5 analyses to achieve a 2RSE external precision of $1.5\,‰$ and ~ 10 analyses for $1.0\,‰$ (2RSE). This would require 2.7 and 5.4 hours, respectively, not including analyses of the reference materials. The practical results for multiple analyses on MORB glasses demonstrate that the values are reproducible within the error given by internal precision, and produce mean δ^{11}B values with 2RSE of $1-2\,‰$ (Fig. 4).

Analytical drift

Drift within individual measurements (internal drift)

The internal precision of an isotope ratio measurement is influenced by the total integration time, as discussed above. It would, therefore, seem logical to extend analyses on low-concentration samples to very long counting times to improve precision. However, such a practice reduces the number of samples that could be analysed in a given time, which has practical and financial drawbacks. More importantly, though, it also introduces additional potential sources of analytical bias. Analyses that sputter the sample for one hour or longer create relatively deep pits potentially leading to a shift in instrumental fractionation over the course of the analysis (Hervig *et al.*, 1992). Previous SIMS studies performing oxygen isotope and trace element analyses recommend not to exceed aspect ratios of the sputter pit (depth divided by diameter) of 0.1 (Schuhmacher *et al.*, 1994) or 0.25 (Valley & Graham, 1991; Hervig *et al.*, 1992). The aspect ratio of the

pits produced by the 40-cycle analyses in our setup after 32 min is ~ 0.1. Longer sputter times with more cycles would increase the aspect ratio. For example, the pit created by a 400-cycle analysis is $\sim 25\,\mu m$ deep with an aspect ratio of ~ 0.8. The shape of the pit is also asymmetrical due to the incidence angle of the primary beam of $\sim 68^{\circ}$. The influence of sputter time or pit aspect ratio on the measured B isotope ratio was not investigated systematically in this study, but it was found that a 400-cycle analysis on glass reference material GOR132-G showed IMF values within 1 ‰ of the value determined from the first 40 analytical cycles only for the first ~ 200 cycles. At that stage, the aspect ratio of the pit is ≥ 0.4 produced after a sputter time of two hours. At an aspect ratio of ≥ 0.5 the IMF value is ~ 2 ‰ lower than the value determined from the first 40 cycles. The B count rate decreased to approximately half of the initial value after 400 cycles. These findings also demonstrate that determination of IMF values from analyses of references materials and analyses of unknown samples need to be completed with the same analytical setup and the same number of analytical cycles.

The setup used in this study uses relatively short total sputter durations of 32 min for a single spot analysis (Table 2). Ion count rates and the $^{11}B/^{10}B$ ratio are monitored over the course of each analysis (Fig. 5). Potential drift in the $^{11}B/^{10}B$ ratio is evaluated through the slope of the linear regression of the isotope ratio over the course of the 39 intensity-corrected measurement cycles (Fig. 5). These slopes are mostly not significantly different from zero within 2 standard errors (Fig. 6). In addition, two important criteria must be fulfilled for a set of analyses that do not show systematic analytical drift during a single anaysis: (1) the slopes for a set of analyses should follow a random distribution that is symmetrical around zero, and (2) the magnitude of the slopes should decrease with increasing count rate and increase with increasing standard deviation, i.e., with worse analytical precision. Both conditions are fulfilled for the set of 221 analyses completed over the course of this study, demonstrating that no systematic drift occurs under the current setup and analytical protocol (Fig. 6).

Long-term drift

Changes in instrumental mass fractionation in SIMS over the duration of several hours or days are observed for O isotope analyses, and require frequent analysis of reference materials and a time-related correction of the measured ratios for the samples (e.g., Valley *et al.*, 1998; Kita *et al.*, 2009). Long-term drift of IMF has been observed to be negligible or within the precision of the analysed reference materials for B isotope analyses in a number of previous studies (Chaussidon *et al.*, 1997; Marschall *et al.*, 2006*b*). In this study, drift of the IMF was observed over the course of one day, with IMF values slowly changing by typically $+$ or $-0.1\,‰/\mathrm{h}$ from early morning to late night. Note that this drift may be positive or negative (Fig. 7), and that the total drift over an entire day never exceeded $1.8\,‰$. Observation and quantification of drift are practically limited by the reproducibility of the analyses of the reference materials. Instrumental drift over the course of one day can be corrected for through the repeated analysis of reference materials throughout the analytical session. Alternatively, the drift-uncorrected IMF values for the entire session may be used, which would increase the uncertainty on IMF from typically $1.5\,‰$ to $\sim 2.4\,‰$ (Fig. 7).

Matrix effects

The matrix effect describes the dependency of the instrumental mass fractionation on the chemical composition or crystallographic structure of the analysed materials. Chemical matrix effects have been reported for a number of trace element and isotope systems and require close chemical matching between standards and samples or a good description of the matrix effect as a function of composition (Shimizu & Hart, 1982; Eiler *et al.*, 1997; Page *et al.*, 2010). Matrix effects for B isotopes have been reported to be very small or negligible for a large range of minerals and glasses with the exception of the NIST glass series SRM 61x and one sample of a Li-rich tourmaline (Chaussidon & Albarède, 1992; Chaussidon *et al.*, 1997; Nakano & Nakamura, 2001; Rosner *et al.*, 2008; Gurenko & Kamenetsky, 2011). Small matrix effects were also reported between amphibole and rhyolitic glass B6 ($2.8 \pm 2.0\,‰$; 1σ), but were insignificant for the pair

phengite and B6 (1.3 ± 2.8 ‰; 1σ; Pabst *et al.*, 2012). In this study, the possible effect of the chemical composition of the investigated material on instrumental fractionation of the two isotopes of B was investigated by comparing IMF values determined for the four different reference materials. These four different glasses vary in composition from komatiitic to rhyolitic with silica contents from ~ 45 to ~ 75 wt% (Table 1).

The recommended δ^{11}B values for these reference glasses are relatively well established and they were repeatedly analysed in a number of laboratories by various methods. However, it should be noted that there are still existing discrepancies between values reported by various laboratories that are larger than the reported precisions (e.g., Gonfiantini *et al.*, 2003). Hence, although many TIMS and ICP-MS laboratories routinely produce B isotope data on silicate minerals and glasses with reported analytical uncertainties of $2\sigma < 0.5$ ‰, reproducibilities including full sample dissolution and chemical B separation are more typical in the range $0.5 - 1$ ‰. Interlaboratory comparison reveals consistencies on the order of only $1.5 - 3.0$ ‰ (Gonfiantini *et al.*, 2003; Tiepolo *et al.*, 2006; Hou *et al.*, 2010; Wei *et al.*, 2013). Consequently, there are relatively large uncertainties on the reported δ^{11}B values, which limits the evaluation of possible SIMS matrix effects. Note that if not taken into account, accumulation of all uncertainties on the reference values can lead to a significant overestimation of SIMS matrix effects.

The results from this study confirm previous results that no significant matrix effects can be detected for the large compositional range of reference glasses (Fig. 9, 10). The differences in IMF among the various materials are well within the repeatibility of the B isotope analyses on these samples; no correlation between IMF and chemical composition was detected (Fig. 9b). The difference in IMF between komatiitic glass GOR132-G and dacitic glass StHs6/80-G is 0.04 ± 1.64 ‰ (2SD). The weighted mean of four sessions for the differences in IMF between komatiitic glass GOR132-G and rhyolitic glass B6 is 0.18 ± 1.36 ‰ (2SD). The difference in IMF between the two komatiitic glasses GOR132-G and GOR128-G is 0.25 ± 1.87 ‰ (2SD). All of these values are insignificant since the uncertainties are much larger than the values.

Note that these errors do not include uncertainties on the reference values, which, if propagated, would make the observed differences even less significant. In conclusion, in the analytical setup used in this

study the potential matrix effect for B isotope analyses for the range of natural glasses with compositions from komatiitic to rhyolitic is much smaller than the reproducibility of the reference glasses. A better quantification of a possible small matrix effect in the low sub-permil range would require more accurate and precise δ^{11}B values for the reference materials.

Reproducibility and accuracy

The primary B isotope standard, boric acid SRM 951 (NIST), cannot be used as a reference material in SIMS to correct instrumental mass fractionation of measurements on silicate glass. Hence, accuracy of the B isotope measurements can only be evaluated relative to secondary reference materials. Uncertainties on the reported δ^{11}B values on those secondary reference materials, therefore, translate into a larger uncertainty on the accuracy of the δ^{11}B values reported from the SIMS laboratory, if more than one reference material is used for calibration. The use of an average IMF value determined from a set of reference materials reduces the dependency on a single reference material and potentially reduces the inaccuracy of the reported δ^{11}B value.

The instrumental mass fractionation over a single session in this study based on all analysed reference materials showed values to be reproducible within ± 1.3 to ± 2.4 ‰ (2RSD) and ± 0.4 to ± 1.1 ‰ (2RSE) for all sessions (Fig. 8). The reproducibility of individual reference materials are in the same range (Fig. 9a). These values are also in the same range as the ones reported in previous studies using various SIMS instruments or LA-ICP-MS (Table 2). For MPI-DING reference glasses GOR128-G, GOR132-G, and StHs6/80-G, the reproducibility of $0.4 - 1.6$ ‰ (2RSD; Fig. 9) is in a similar range as the internal precision on these materials ($0.5 - 1.9$ ‰; both median and mean are 1.0 ‰).

Conclusions

The enhanced transmission and stability of the Cameca 1280 setup used at NENIMF (the Woods Hole SIMS facility) in the course of this study led to an improvement of precision and reduced instrument drift, surface contamination and analysis time compared to earlier studies. Accuracy, reproducibility, precision, matrix effects, contamination and machine background were quantified and their influence on samples with low B concentrations was determined. Single analyses were completed with a spatial resolution of $30 \times 30\,\mu m$ within 32 min.

The accuracy of the SIMS analyses for multiple analyses of a homogenous material is determined by the reproducibility of all analyses within a given analytical session ($\sim 2-5$ days), and was ± 0.4 to $\pm 2.3\,‰$ (2RSD). Precision of a single B isotope analysis of basaltic glass with $1\,\mu g/g$ B is determined by Poisson statistics and is $3.1\,‰$ (2RSD). Analysis of homogenous basaltic glass with $1\,\mu g/g$ B require ~ 5 analyses to achieve a 2RSE precision of better than $\pm 1.5\,‰$. At concentrations exceeding $\sim 20\,\mu g/g$, internal precision reaches a lower limit of $0.5\,‰$ (2RSE).

Chemical matrix effects are too small to be quantified, i.e. no significant differences in instrumental mass fractionation were observed (even on the $1-\sigma$ level) for the range of investigated glass compositions ranging from komatiitic to rhyolitic. The analysis are demonstrated to show no systematic internal drift. Long-term drift over the course of a day is limited ($< 1.8\,‰$ throughout one day) and can be quantified and corrected for through multiple analyses of reference glasses. Surface contamination can contribute bias. However, this was negligible ($< 0.1 \pm 0.2\,‰$) in samples exceeding $2.5\,\mu g/g$ boron. At the low end of concentrations found in MORB glasses ($0.4\,\mu g/g$) the bias introduced by surface contamination is still small ($0.6 \pm 1.1\,‰$) compared to precision at that concentration ($4-5\,‰$; 2RSE).

In summary, the newly developed setup at NENIMF is capable of determining the B isotopic composition of natural volcanic glasses, including basaltic glasses with very low B abundances such as depleted MORB glass. Precision, accuracy and reproducibility of better than $1.5\,‰$ (2RSE) is achieved, including possible

sources of error, such as surface contamination, drift and matrix effects. Samples with less than $\sim 4\,\mu g/g$ require several analyses to achieve this precision, but analysis time is relatively short at ~ 30 min per spot.

The method presented here constitutes an improvement of analytical uncertainty by a factor of approximately two to four, while reducing the analysis time by a factor of three compared to previously reported ion microprobe protocols. Analytical uncertainties are comparable to those of laser-ablation multiple-multiplier inductively coupled plasma mass spectrometry, but with the analysed area reduced by two to three orders of magnitude and the analysed sample volume reduced by three to four orders of magnitude. The method presented here, thus, not only provides the analytical capabilities to investigate MORB glasses at a geologically meaningful level of uncertainty, but also to investigate spatially restricted samples, such as melt inclusions and crystallite-rich glasses, which are not accessible by methods other than SIMS.

Acknowledgments

We would like to thank Nobu Shimizu for many insightful discussions on this topic over the past three years, and we are thankful to Thomas Ludwig (Heidelberg) for detailed discussions and an informal review of the manuscript. We thank Tim Elliott for providing a selection of MORB glass samples. Two anonymous reviews and editorial handling by Jon Woodhead are acknowledged. This study was financially supported by the NSF ocean sciences program (OCE grant 1232996 to Dorsey Wanless and HRM). Ion microprobe analyses at the Northeast National Ion Microprobe Facility at Woods Hole Oceanographic Institution were partially subsidized by the Instrumentation and Facilities Program, Division of Earth Sciences, National Science Foundation (grants 1035310 and 1258876).

References

Catanzaro, E. J., Champion, C. E., Garner, E. L., Marinenko, G., Sappenfield, K. M. & Shields, W. R. (1970) Boric acid: isotopic and assay standard reference materials. *National Bureau of Standards (US) Special*

Publications **260-17**: 1–71

Chaussidon, M. & Albarède, F. (1992) Secular boron isotope variations in the continental crust: an ion microprobe study. *Earth and Planetary Science Letters* **108**: 229–241

Chaussidon, M. & Jambon, A. (1994) Boron content and isotopic composition of oceanic basalts: Geochemical and cosmochemical implications. *Earth and Planetary Science Letters* **121**: 277–291

Chaussidon, M. & Marty, B. (1995) Primitive boron isotope composition of the mantle. *Science* **269**: 383–386

Chaussidon, M., Robert, F., Mangin, D., Hanon, P. & Rose, E. F. (1997) Analytical procedures for the measurement of boron isotope composition by ion microprobe in meteorites and mantle rocks. *Geostandards Newsletter* **21**: 7–17

Chaussidon, M., Robert, F. & McKeegan, K. D. (2006) Li and B isotopic variations in an Allende CAI: Evidence for the in situ decay of short-lived ^{10}Be and for the possible presence of the short-lived nuclide ^{7}Be in the early solar system. *Geochimica et Cosmochimica Acta* **70**: 224–245

Darbouret, D. & Kano, I. (2000) Ultrapure water blank for boron trace analysis. *Journal of Analytical Atomic Spectrometry* **15**: 1395–1399

Domanik, K. J., Hervig, R. L. & Peacock, S. M. (1993) Beryllium and boron in subduction zone minerals: an ion microprobe study. *Geochimica et Cosmochimica Acta* **57**: 4997–5010

Eiler, J. M., Graham, C. M. & Valley, J. W. (1997) SIMS analysis of oxygen isotopes: matrix effects in complex minerals and glasses. *Chemical Geology* **138**: 221–244

Fitzsimons, I. C. W., Harte, B. & Clark, R. M. (2000) SIMS stable isotope measurement: counting statistics and analytical precision. *Mineralogical Magazine* **64**: 59–83

Gonfiantini, R., Tonarini, S., Gröning, M., Adorni-Braccesi, A., Al-Ammar, A. S., Astner, M., Bächler, S., Barnes, R. M., Basset, R. L., Cocherie, A., Deyhle, A., Dini, A., Ferrara, G., Gaillardet, J., Grimm, J., Guerrot, C., Krähenbühl, U., Layne, G., Lemarchand, D., Meixner, A., Northington, D. J., Pennisi, M., Reitznerová, E., Rodushkin, I., Sugiura, N., Surberg, R., Tonn, S., Wiedenbeck, M., Wunderli, S., Xiao, Y. & Zack, T. (2003) Intercomparison of boron isotope and concentration measurements. Part II: evaluation of results. *Geostandards Newsletter* **27**: 41–57

Gurenko, A. A. & Kamenetsky, V. S. (2011) Boron isotopic composition of olivine-hosted melt inclusions from Gorgona komatiites, Colombia: new evidence supporting wet komatiite origin. *Earth and Planetary Science Letters* **312**: 201–212

Hervig, R. L. (2002) Analyses of geological materials for boron by secondary ion mass spectrometry. In: Grew, E. S. & Anovitz, L. M. (eds.) *Boron: mineralogy, petrology and geochemistry*, vol. 33 of *Reviews in Mineralogy*, chap. 16, 789–803, Mineralogical Society of America, Washington, DC, 2^{nd} edn.

Hervig, R. L., Williams, P., Thomas, R. M., Schauer, S. N. & Steele, I. M. (1992) Microanalysis of oxygen isotopes in insulators by secondary ion mass spectrometry. *International Journal of Mass Spectrometry* **120**: 45–63

Hervig, R. L., Mazdab, F. K., Williams, P., Guan, Y., Huss, G. R. & Leshin, L. A. (2006) Useful ion yields for Cameca IMS 3f and 6f SIMS: limits on quantitative analysis. *Chemical Geology* **227**: 83–99

Hoppe, P., Goswami, J. N., Krähenbühl, U. & Marti, K. (2001) Boron in chondrules. *Meteoritics and Planetary Science* **36**: 1331–1343

Hou, K. J., Li, Y. H., Xiao, Y. K., Liu, F. & Tian, Y. R. (2010) In situ boron isotope measurements of natural geological materials by LA-MC-ICP-MS. *Chinese Science Bulletin* **55**: 3305–3311

Jochum, K. P., Dingwell, D. B., Rocholl, A., Stoll, B., Hofmann, A., Becker, S., Bessette, D., Dietze, H. J., Dulski, P., Erzinger, J., Hellebrand, E., Hoppe, P., Horn, I., Janssens, K., Jenner, G. A., Klein, M., Mc-

Donough, W. F., Maetz, M., Mezger, K., Münker, C., Nikogosian, I. K., Pickhardt, C., Raczek, I., Rhede, D., Seufert, H. M., Simakin, S. G., Sobolev, A. V., Spettel, B., Straub, S., Vincze, L., Wallianos, A., Weckwerth, G., Weyer, S., Wolf, D. & Zimmer, M. (2000) The preparation and preliminary characterisation of eight geological MPI-DING reference glasses for in-situ microanalysis. *Geostandards Newsletter* **24**: 87–133

Jochum, K. P., Stoll, B., Herwig, K., Willbold, M., Hofmann, A., Amini, M., Aarburg, S., Abouchami, W., Hellebrand, E., Mocek, B., Raczek, I., Stracke, A., Alard, O., Bouman, C., Becker, S., Dücking, M., Brätz, H., Klemd, R., de Bruin, D., Canil, D., Cornell, D., de Hoog, C. J., Dalpé, C., Danyushevsky, L. V., Eisenhauer, A., Gao, Y., Snow, J. E., Groschopf, N., Günther, D., Latkoczy, C., Giullong, M., Hauri, E. H., Höfer, H. E., Lahaye, Y., Horz, K., Jacob, D. E., Kasemann, S. A., Kent, A. J. R., Ludwig, T., Zack, T., Mason, P. R. D., Meixner, A., Rosner, M., Misawa, K., Nash, B. P., Pfänder, J. A., Premo, W. R., Sun, W. D., Tiepolo, M., Vannucci, R., Vennemann, T., Wayne, D. & Woodhead, J. D. (2006) MPI-DING reference glasses for in situ microanalysis: New reference values for element concentrations and isotope ratios. *Geochemistry, Geophysics, Geosystems (G^3)* **7**: Q02 008, doi:10.1029/2005GC001 060

Kent, A. J. R. & Rossman, G. R. (2002) Hydrogen, lithium, and boron in mantle-derived olivine: The role of coupled substitutions. *American Mineralogist* **87**: 1432–1436

Kita, N. T., Ushikubo, T., Fu, B. & Valley, J. W. (2009) High precision SIMS oxygen isotope analysis and the effect of sample topography. *Chemical Geology* **264**: 43–57

Leeman, W. P. & Sisson, V. B. (2002) Geochemistry of boron and its implications for crustal and mantle processes. In: Grew, E. S. & Anovitz, L. M. (eds.) *Boron: mineralogy, petrology and geochemistry*, vol. 33, 645–708, Mineralogical Society of America, Washington, DC, 2^{nd} edn.

Ludwig, T., Marschall, H. R., Pogge von Strandmann, P. A. E., Shabaga, B. M., Fayek, M. & Hawthorne, F. C. (2011) A secondary ion mass spectrometry (SIMS) re-evaluation of B and Li isotopic compositions of Cu-bearing elbaite from three global localities. *Mineralogical Magazine* **75**: 2485–2494

490 Marschall, H. R. & Ludwig, T. (2004) The Low-Boron contest: minimising surface contamination and
491 analysing boron concentrations at the ng/g-level by secondary ion mass spectrometry. *Mineralogy and*
492 *Petrology* **81**: 265–278

493 Marschall, H. R., Altherr, R., Ludwig, T., Kalt, A., Gméling, K. & Kasztovszky, Z. (2006*a*) Partitioning
494 and budget of Li, Be and B in high-pressure metamorphic rocks. *Geochimica et Cosmochimica Acta* **70**:
495 4750–4769

496 Marschall, H. R., Ludwig, T., Altherr, R., Kalt, A. & Tonarini, S. (2006*b*) Syros metasomatic tourmaline:
497 evidence for very high-δ^{11}B fluids in subduction zones. *Journal of Petrology* **47**: 1915–1942

498 Müller, A., Wiedenbeck, M., van der Kerkhof, A. M., Kronz, A. & Simon, K. (2003) Trace elements in
499 quartz – a combined electron microprobe, secondary ion mass spectrometry, laser-ablation ICP-MS, and
500 cathodoluminescence study. *European Journal of Mineralogy* **15**: 747–763

501 Nakano, T. & Nakamura, E. (2001) Boron isotope geochemistry of metasedimentary rocks and tourmalines
502 in a subduction zone metamorphic suite. *Physics of the Earth and Planetary Interiors* **127**: 233–252

503 Ogliore, R. C., Huss, G. R. & Nagashima, K. (2011) Ratio estimation in SIMS analysis. *Nuclear Instruments*
504 *and Methods in Physics Research B* **269**: 1910–1918

505 Ottolini, L., Le Fèvre, B. & Vannucci, R. (2004) Direct assessment of mantle boron and lithium contents and
506 distribution by SIMS analyses of peridotite minerals. *Earth and Planetary Science Letters* **228**: 19–36

507 Pabst, S., Zack, T., Savov, I. P., Ludwig, T., Rost, D., Tonarini, S. & Vicenzi, E. P. (2012) The fate of sub-
508 ducted oceanic slabs in the shallow mantle: insights from boron isotopes and light element composition
509 of metasomatized blueschists from the Mariana forearc. *Lithos* **132-133**: 162–179

510 Page, F. Z., Kita, N. T. & Valley, J. W. (2010) Ion microprobe analysis of oxygen isotopes in garnets of
511 complex chemistry. *Chemical Geology* **270**: 9–19

Palmer, M. R. & Swihart, G. H. (1996) Boron isotope geochemistry: an overview. In: Grew, E. S. & Anovitz, L. M. (eds.) *Boron: mineralogy, petrology and geochemistry*, vol. 33 of *Reviews in Mineralogy*, chap. 13, 709–740, Mineralogical Society of America, Washington, DC, 1^{st} edn.

Rosner, M. & Meixner, A. (2004) Boron isotopic composition and concentration of ten geological reference materials. *Geostandards And Geoanalytical Research* **28**: 431–441

Rosner, M., Wiedenbeck, M. & Ludwig, T. (2008) Composition-induced variations in SIMS instrumental mass fractionation during boron isotope ratio measurements of silicate glasses. *Geostandards And Geoanalytical Research* **32**: 27–38

le Roux, P. J., Shirey, S. B., Benton, L., Hauri, E. H. & Mock, T. D. (2004) In situ, multiple-multiplier, laser ablation ICP-MS measurement of boron isotopic composition (δ^{11}B) at the nanogram level. *Chemical Geology* **203**: 123–138

Ryan, J. G. & Langmuir, C. H. (1993) The systematics of boron abundances in young volcanic rocks. *Geochimica et Cosmochimica Acta* **57**: 1489–1498

Schuhmacher, M., de Chambost, E., McKeegan, K. D., Harrison, T. M. & Midgeon, H. (1994) In-situ dating of zircon with the Cameca ims-1270. In: Benninghoven, A., Nihel, Y., Shimizu, R. & Werner, H. W. (eds.) *Secondary Ion Mass Spectrometry*, 919–922, Wiley, New York

Shaw, A. M., Hauri, E. H., Behn, M. D., Hilton, D. R., Macpherson, C. G. & Sinton, J. M. (2012) Long-term preservation of slab signatures in the mantle inferred from hydrogen isotopes. *Nature Geoscience* **5**: 224–228

Shaw, D. M., Higgins, M. D., Truscott, M. G. & Middleton, T. A. (1988) Boron contamination in polished thin sections of meteorites: Implications for other trace-element studies by alpha-track image or ion microprobe. *American Mineralogist* **73**: 894–900

534 Shimizu, N. & Hart, S. R. (1982) Isotope fractionation in secondary ion mass spectometry. *Journal of*
535 *Applied Physics* **53**: 1303–1311

536 Spivack, A. J. & Edmond, J. M. (1987) Boron isotope exchange between seawater and the oceanic crust.
537 *Geochimica et Cosmochimica Acta* **51**: 1033–1043

538 Sugiura, N., Shuzou, Y. & Ulyanov, A. (2001) Beryllium-boron and aluminium-magnesium chronology of
539 calcium-aluminium-rich inclusions in CV chondrites. *Meteoritics and Planetary Science* **36**: 1397–1408

540 Tiepolo, M., Bouman, C., Vannucci, R. & Schwieters, J. (2006) Laser ablation multicollector ICP-MS
541 determination of δ^{11}B in geological samples. *Applied Geochemistry* **21**: 788–801

542 Tonarini, S., Pennisi, M., Adorno-Braccesi, A., Dini, A., Ferrara, G., Gonfiantini, R., Wiedenbeck, M. &
543 Gröning, M. (2003) Intercomparison of boron isotope and concentration measurements. Part I: selection,
544 preparation and homogeneity tests of the intercomparison materials. *Geostandards Newsletter* **27**: 21–39

545 Turner, S., Tonarini, S., Bindemann, I., Leeman, W. P. & Schaefer, B. F. (2007) Boron and oxygen isotope
546 evidence for recycling of subducted components over the past 2.5 Gyr. *Nature* **447**: 702–705

547 Valley, J. W. & Graham, C. M. (1991) Ion microprobe analysis of oxygen isotope ratios in granulite facies
548 magnetites: diffusive exchange as a guide to cooling history. *Contributions to Mineralogy and Petrology*
549 **109**: 38–52

550 Valley, J. W., Graham, C. M., Harte, B., Eiler, J. M. & Kinny, P. D. (1998) Ion microprobe analysis of
551 oxygen, carbon, and hydrogen isotope ratios. In: McKibben, M. A., Shanks, W. C. & Ridley, W. I. (eds.)
552 *Applications of microanalytical techniques to understanding mineralizing processes*, vol. 7 of *Reviews in*
553 *Economic Geology*, 73–98, Society of Economic Geologists

554 Wei, G., Wei, J., Liu, Y., Ke, T., Ren, Z., Ma, J. & Xu, Y. (2013) Measurement on high-precision boron iso-
555 tope of silicate materials by a single column purification method and MC-ICP-MS. *Journal of Analytical*
556 *Atomic Spectrometry* **28**: 606–612

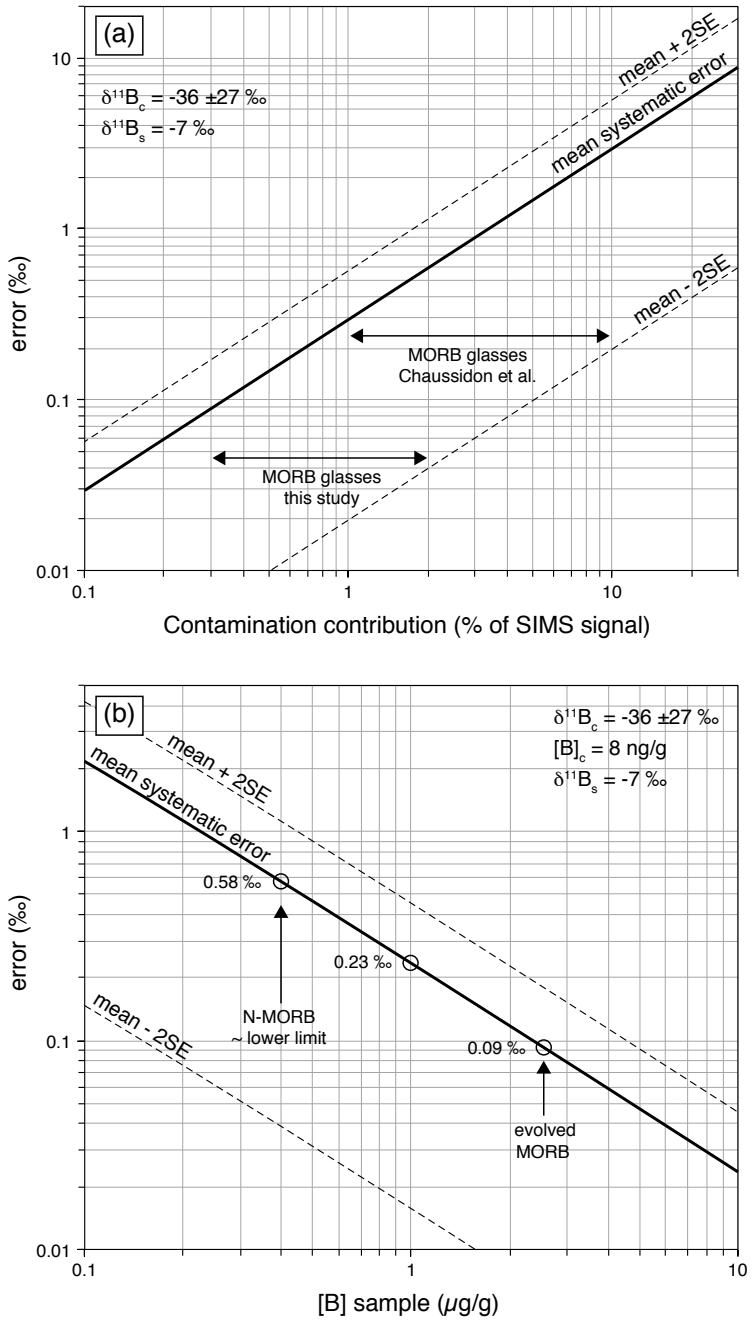

Fig. 1 (a) Systematic error introduced by surface and machine boron contamination as a function of the proportion of the contamination in the SIMS signal (sample $\delta^{11}B_s = -7.0‰$; contamination $\delta^{11}B_c = -36 \pm 27‰$). The continuous black line shows the systematic error, while the dashed lines shows the uncertainty (2 standard error) on that systematic error. The contribution of surface contamination during MORB glass analysis in this study was determined to be $0.3 - 2.0\%$, while it was estimated at approximately five times higher in one previous study (Chaussidon *et al.*, 1997, no other studies have systematically quantified the contamination). **(b)** Systematic error introduced by boron contamination in this study as a function of sample boron concentration, assuming $8\,ng/g$ contamination (B isotopic compositions as in (a)). MORB glass typically contains $0.4 - 2.5\,\mu g/g$ B. The systematic error expected from surface contamination at $1\,\mu g/g$ concentration in this study is $+0.23‰$ (2SE: $+0.02$ to $+0.45‰$). Note the large uncertainty on the error.

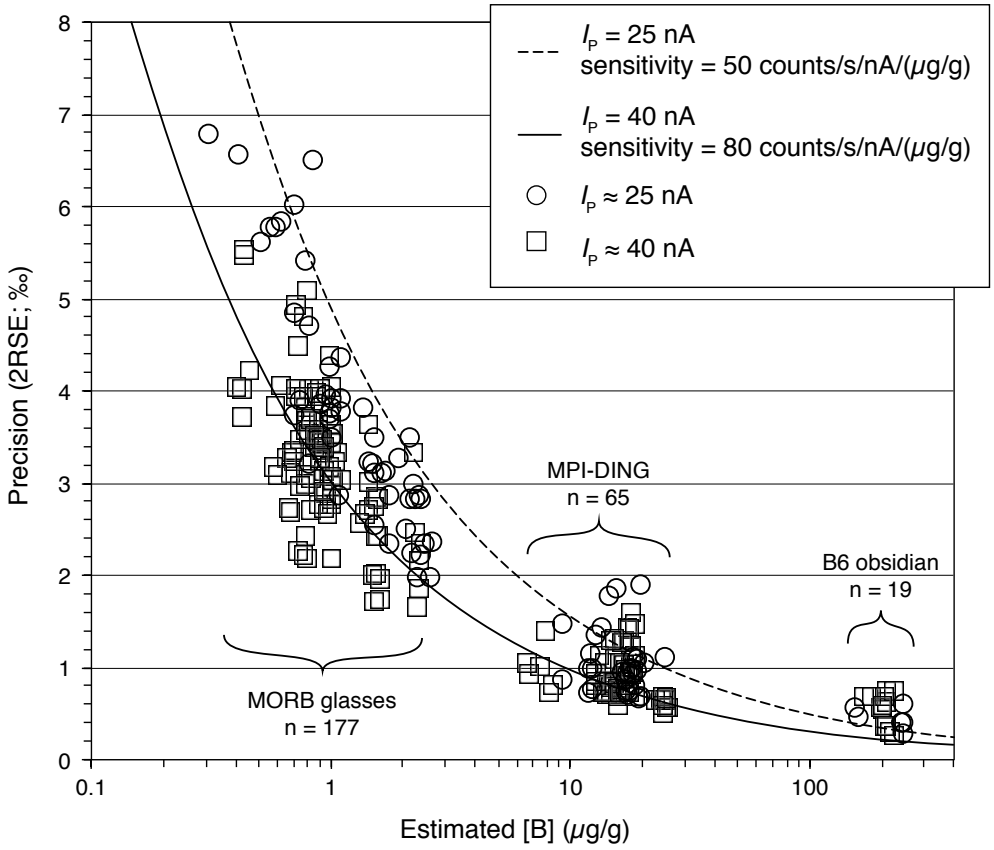

Fig. 2 Internal precision of individual B isotope analyses, expressed as two times the relative standard error, as a function of boron concentration (estimated from ^{11}B count rates) for reference materials and a range of MORB glasses. Two different primary beam currents were used, and sensitivity varied between sessions. Observed precision and precisions predicted from Poisson statistics (e.g., Fitzsimons *et al.*, 2000) agree well at low concentrations, while counting statistics is not the limiting factor at concentrations $> 20\,\mu g/g$ where internal precision reaches a practical lower limit of $\sim 0.5\,‰$ (2RSE).

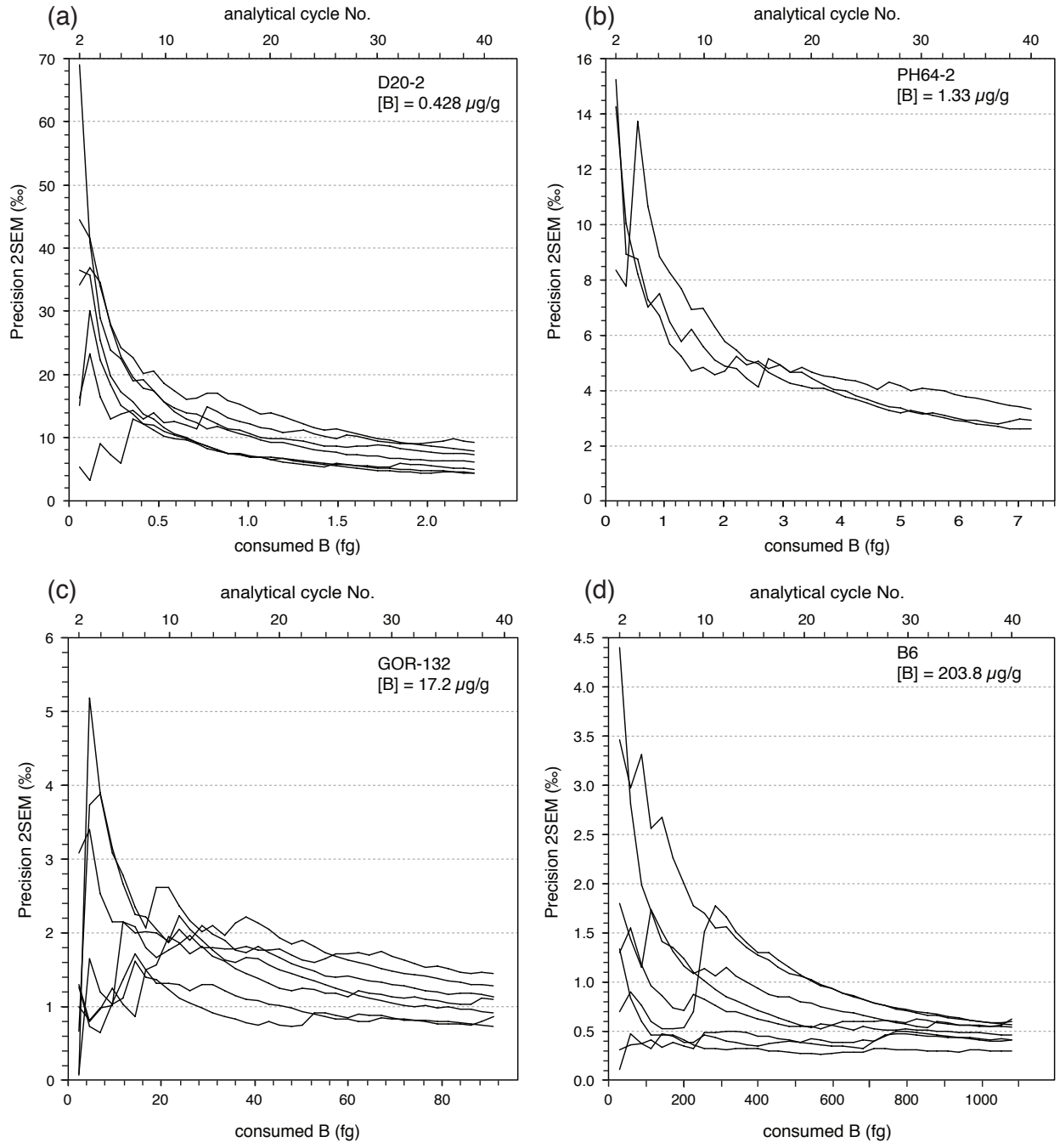

Fig. 3 Internal precision of individual B isotope analyses, expressed as two times the relative standard error, as a function of boron consumed during the analysis ($1\,\mathrm{fg} = 10^{-15}\,\mathrm{g}$) for reference materials and two different MORB glasses. The amount of boron consumed during presputtering is not included in order to facilitate comparison among the samples. The number of analytical cycles are given on the secondary x-axis on top. Note the different scales on x and y axes among figures (a) to (d).

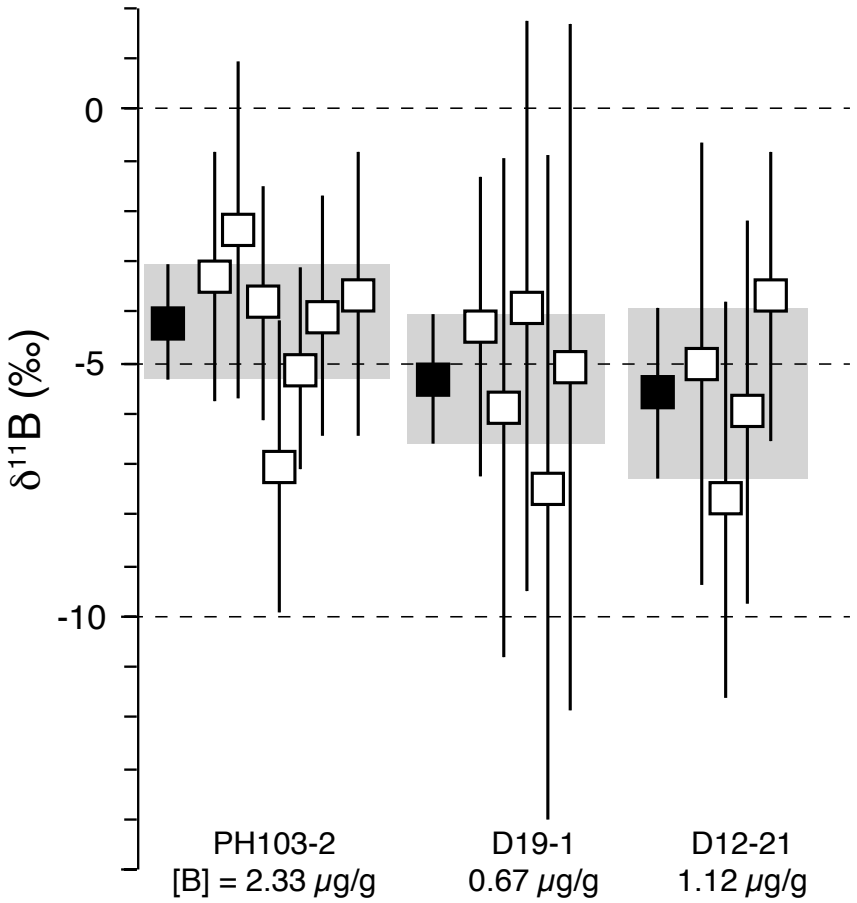

Fig. 4 Repeated measurements of B isotopic composition of three different MORB glass samples with B concentrations between 0.67 and 2.33 $\mu g/g$. White squares mark individual measurements with internal 2SD error bars; solid squares mark sample means with 2SE error bars also highlighted by grey fields.

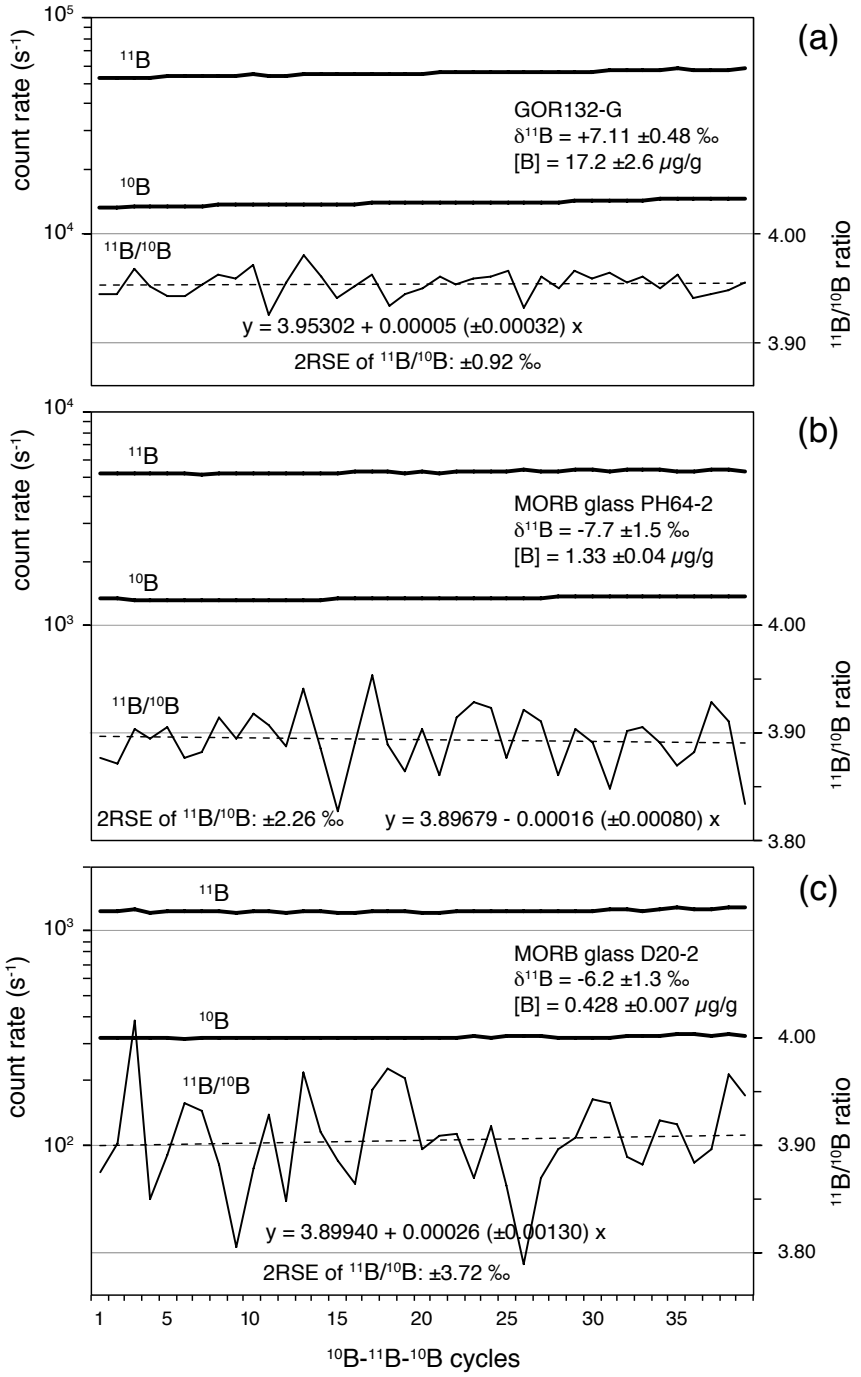

Fig. 5 Three examples of typical ^{11}B and ^{10}B signals and $^{11}B/^{10}B$ ratios over a 40-cycles analysis (intensity-corrected to 39 isotope ratios): **(a)** Reference material MPI-DING glass GOR132-G, **(b)** MORB glass PH64-2 with $[B] = 1.33\,\mu g/g$, and **(c)** MORB glass D20-2 with $[B] = 0.428\,\mu g/g$. The dashed lines and the linear equations in each diagram show the linear regression of the isotope ratios over the analyses, including 2SE on the slope of this regression. Note that the slopes of the regression lines are not significantly different form zero and are unsystematic with positive and negative values.

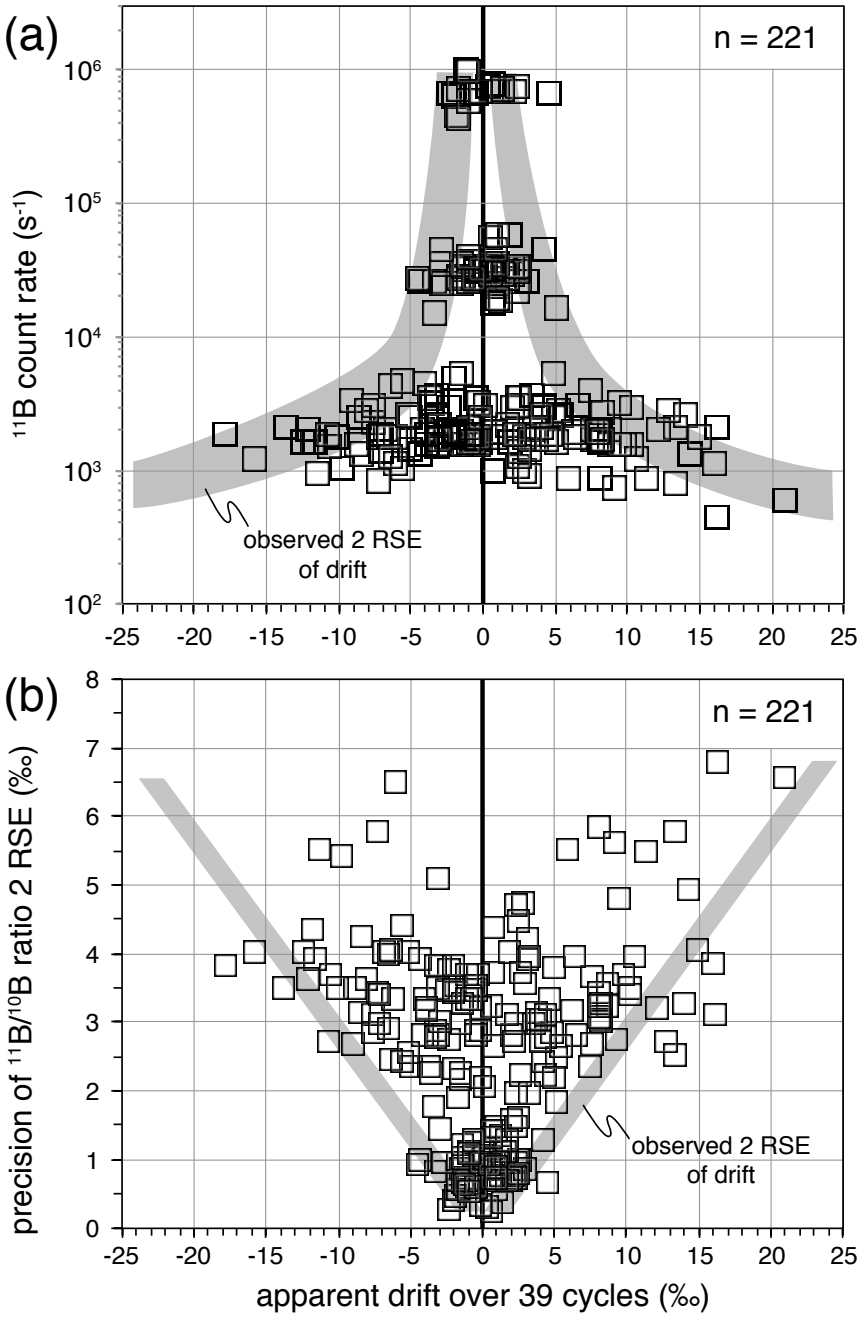

Fig. 6 Apparent drift during single spot analyses as calculated from the slope of the linear regression through the $^{11}B/^{10}B$ ratios over the 40-cycles analyses intensity-corrected to 39 isotope ratios (see Fig. 5). The observed drift is not systematic and shows a symmetric distribution between positive and negative slopes centered around 0, and the magnitudes of the slopes decrease with **(a)** ^{11}B count rate and **(b)** analytical precision. The grey fields mark the 2SE of the slope of the linear regression lines as observed from the same analyses. Only analyses that plot outside the grey envelopes show > 2SE significant drift.

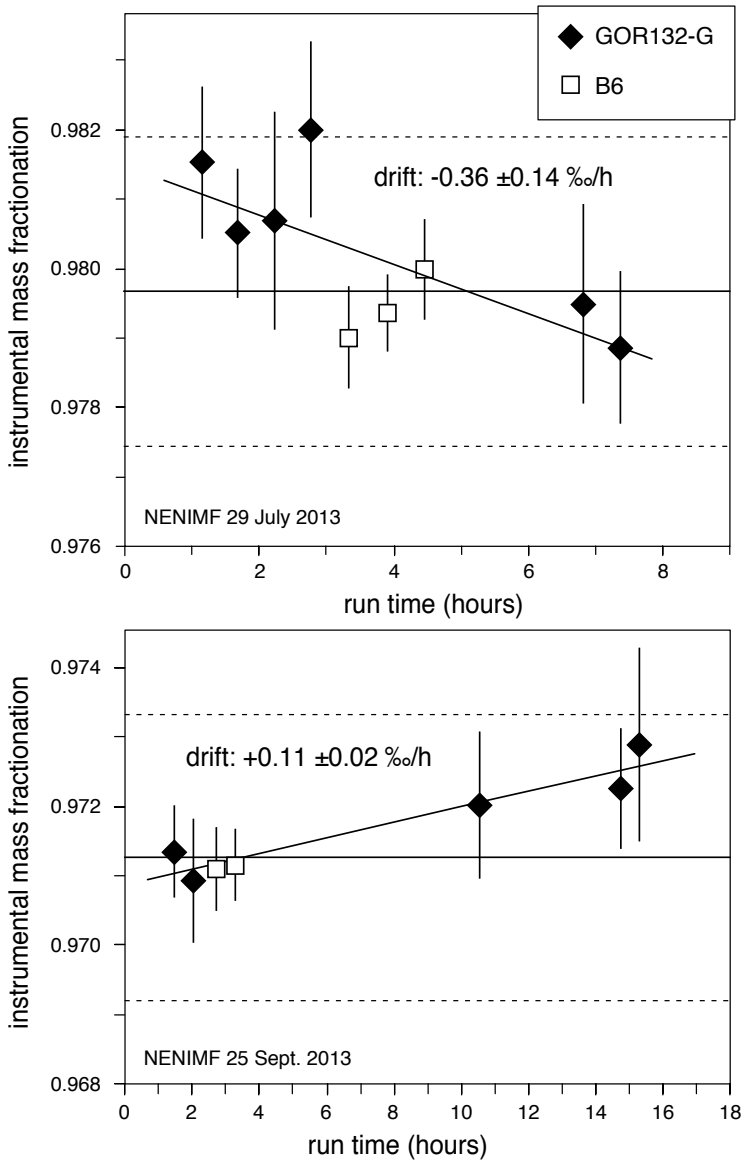

Fig. 7 Two examples of drift of instrumental mass fractionation over the course of an analytical day (run time given in hours). The IMF drift over one day was typically between -0.4 and $+0.3\,‰/\mathrm{h}$, and never exceeded $1.8\,‰$ in total over the course of one day. Without any drift correction, all analysis of one session (up to 6 days) vary around one mean value with a variation of less than $\pm 2.4\,‰$ (2SD) during an entire session, as indicated by the solid and dashed horizontal lines, respectively.

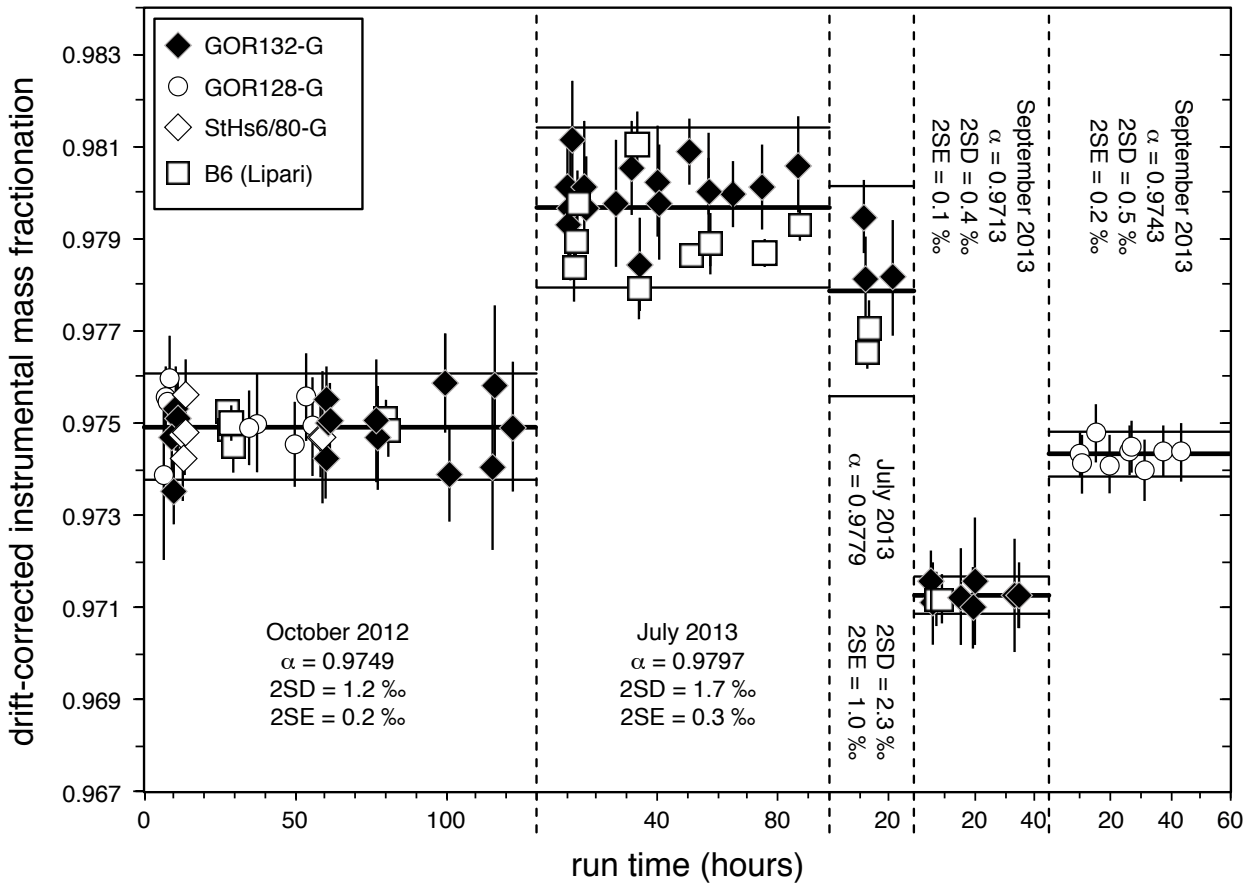

Fig. 8 Instrumental mass fractionation (corrected for intra-day instrumental drift) during five different analytical sessions over the course of one year, plotted against run time of each session. The longest session lasted one week. Reproducibility of instrumental mass fractionation was accurate within ±0.4 to ±2.3‰ (2SD) as demonstrated through repeated measurements of a number of reference materials.

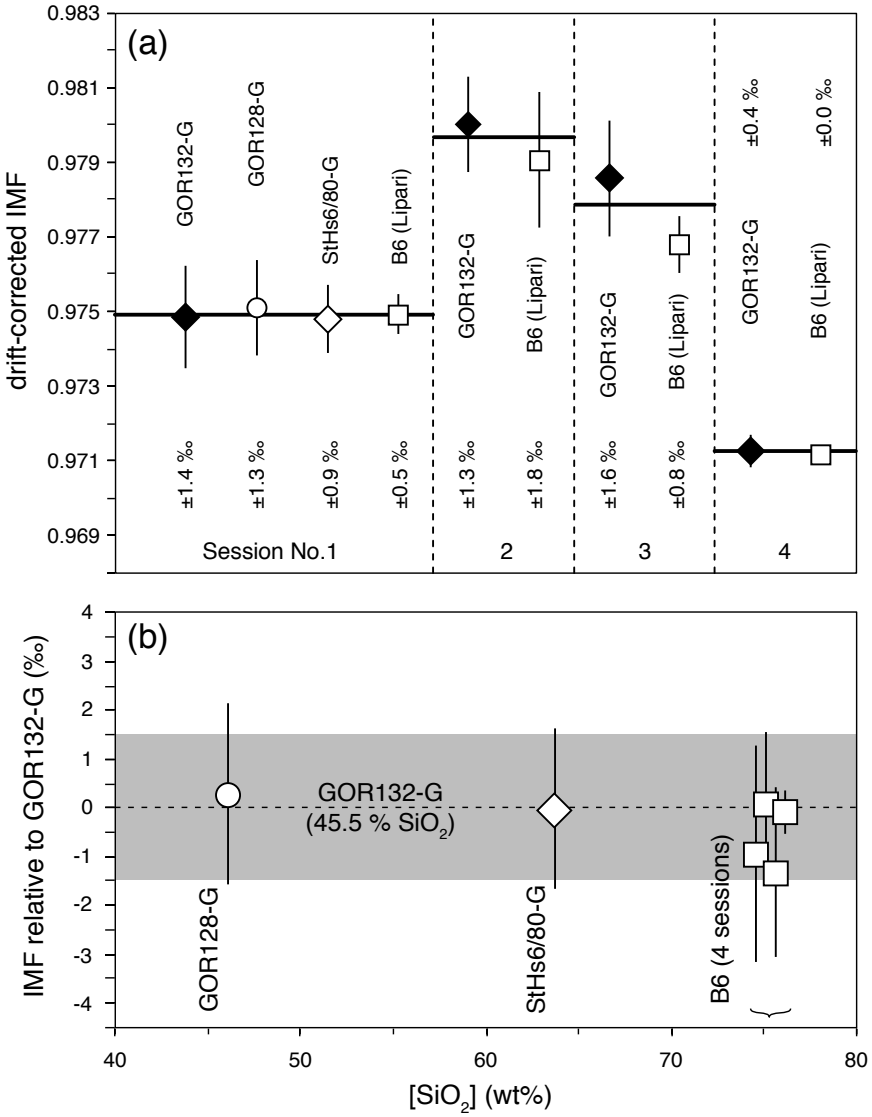

Fig. 9 (a) Drift-corrected instrumental mass fractionation (IMF) in four different analytical sessions for four different reference materials. IMF may vary between sessions, but no significant differences in IMF between different materials were observed. The values given depict reproducibilities of the materials throughout the session (2SD). **(b)** Drift-corrected IMF relative to reference material MPI-DING glass GOR132-G plotted versus silica content. No significant difference was observed in the IMF between reference materials, despite a large compositional range from komatiitic to rhyolitic composition. Hence, no compositional matrix effect can be detected for B isotope analyses in our SIMS lab for glasses of natural composition ranging from komatiite to rhyolite. Note that the propagated errors do not include uncertainties (precision or accuracy) on the reference values. The grey bar represents typical reproducibility (2SD) of GOR132-G.

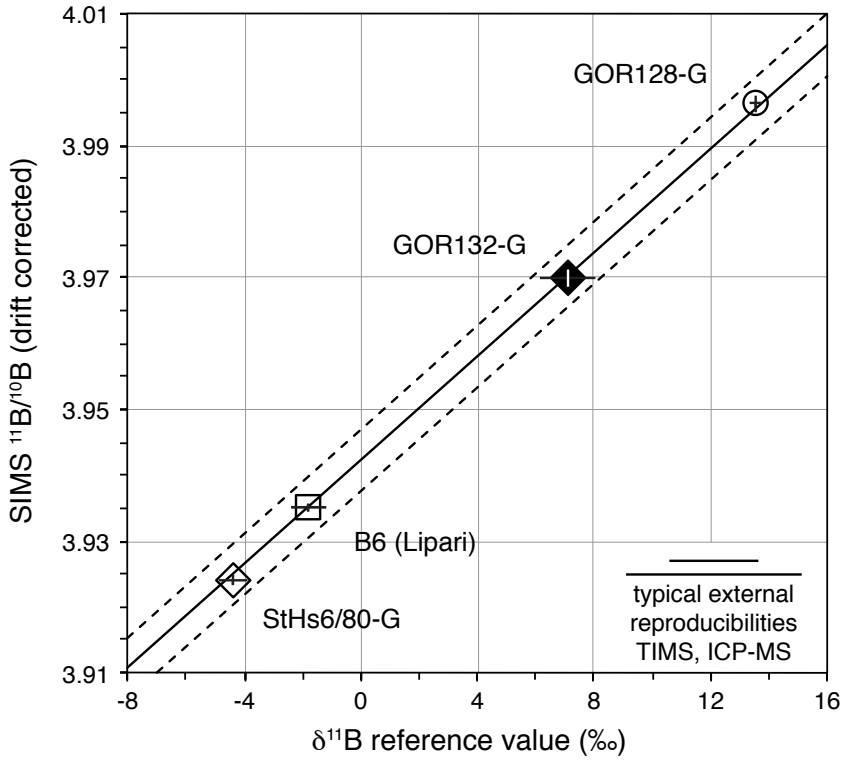

Fig. 10 Drift-corrected $^{11}B/^{10}B$ ratio versus recommended $\delta^{11}B$ values for four different glass reference materials. The reference values have a typical precision of ± 0.5 permil. However, interlab comparison studies show that the accuracy of the TIMS and ICP-MS analyses are more typically in the range of $\pm 1.5 - 3$ permil, as indicated by the bars in the lower right corner. The diagonal black line indicates constant instrumental mass fractionation ($\alpha = 0.9749 \pm 0.0013$). Note that the reference materials range from komatiitic to rhyolitic in composition, and no matrix effect is detectable among these materials. This plot also shows that the IMF is independent of the absolute $^{11}B/^{10}B$ ratio.

Table 1 Reference materials used in this study

Name	Locality	Composition	[SiO_2] (wt%)	[B] ($\mu g/g$)	2SD	$\delta^{11}B$ (‰)	2SD	References
MPI-DING glasses								
GOR128-G	Gorgona	komatiite	46.1	23.5	2.8	+13.55	0.21	[1,2,3]
GOR132-G	Gorgona	komatiite	45.5	17.2	2.6	+7.11	0.97	[1,2,3]
StHs6/80-G	Mt St. Helens	dacite	63.7	11.8	1.3	-4.48	0.29	[1,2,3,4]
IAEA reference glass								
B6	Lipari	rhyolite	75.2	203.8	8.9	-1.79	0.6	[4,5,6,7]

All listed boron isotope values are values determined by P-TIMS. Uncertainties represent 2SD on the reported results and do not include uncertainties from full repeats including sample dissolution or from interlaboratory differences, which are typically on the order of $\pm 1.5 - 3$ ‰. References are: [1] Jochum *et al.* (2006), [2] Rosner & Meixner (2004), [3] Tiepolo *et al.* (2006), [4] Rosner *et al.* (2008), [5] Gonfiantini *et al.* (2003), [6] Wei *et al.* (2013), [7] Hou *et al.* (2010).

Table 2 Uncertainties of B isotope analysis in this study and published studies

Study	Instrument	Detector(s)	Precision of single analysis at [B] = 1 μg/g	Reproducibility of reference materials per session (2SD)	Contamination and background (apparent concentr.)	(system. error)	Spatial resolution (μm)	Analysis time per spot (min)
Secondary-ion mass spetrometry								
this study	Cameca 1280	single multiplier	±3.1‰	0.4 – 2.3‰	3 – 8 ng/g	0.02 – 1.1‰	30 × 30	32
G&K11	Cameca 1280	single multiplier	±5.5‰	1.5 – 3.0‰	not determined		30 × 30	90
CH06	Cameca 1270	single multiplier	∼ ±5‰	1.9 – 3.0‰	not determined		∼ 20 (diameter)	105
CH97	Cameca 3f	single multiplier	±5.7‰	0.9 – 4.4‰	10 – 50 ng/g	± < 3‰	100 (diameter)	90
H01	Cameca 3f	single multiplier	±12.9‰	∼ 3.0‰	not determined		30 (diameter)	90
S01	Cameca 6f	single multiplier	±6.6‰	4.7‰	not determined		∼ 20 (diameter)	40
Laser-Ablation-Multiple-Multiplier-ICP-MS								
leR04	VG Elemental + Nd-YAG laser	two multipliers	±3.6‰	0.8 – 1.0‰	not determined		1650 × 500	6

Listed studies are: G&K11 Gurenko & Kamenetsky (2011) (WHOI prior to 2010); CH06 Chaussidon *et al.* (2006) (CRPG, Nancy); CH97 Chaussidon & Jambon (1994), Chaussidon *et al.* (1997) (CRPG, Nancy); H01 Hoppe *et al.* (2001) (MPI, Mainz); S01 Sugiura *et al.* (2001) (Univ. Tokyo); leR04 le Roux *et al.* (2004) (DTM, Washington D.C.). Note that some of the values listed here are not listed in the original papers, but had to be reconstructed from the given values in the analytical sections and from error bars given in diagrams and converted to 2 standard deviation and 2 standard error, respectively, for this comparison. Values for single analysis precision are average values for the different methods and laboratories.